We are IntechOpen, the world's leading publisher of Open Access books Built by scientists, for scientists

4,800
Open access books available

122,000
International authors and editors

135M
Downloads

Our authors are among the

154
Countries delivered to

TOP 1%
most cited scientists

12.2%
Contributors from top 500 universities

CLARIVATE ANALYTICS
BOOK CITATION INDEX
INDEXED

WEB OF SCIENCE™

Selection of our books indexed in the Book Citation Index
in Web of Science™ Core Collection (BKCI)

Interested in publishing with us?
Contact book.department@intechopen.com

An Analysis of Software and Hardware Development in the PMU-Based Technology and Suggestions Regarding Its Implementation in the Polish Power Grid

Michał Szewczyk

Abstract

The ongoing evolution of electric power systems (EPS), especially distribution systems within the EPS structure, is driven by the implementation of the smart grid framework. This requires new approaches and technologies to continue ensuring a reliable and secure supply to end users. Fluctuating output from solar photovoltaic and wind plants can cause voltage and power variations in the feeders. In the power grid framework, phasor measurement units (PMUs) are recognized to be an invaluable aid in ensuring the secure operation and stability of transmission systems. The synchrophasor technique requires a high-accuracy time stamping of all the measurements within the analyzed power system area. It must be emphasized that the harmonic injection from power electronic components such as fluorescent lighting, computers, and power inverters of motors and generators can increase total harmonic distortion (THD) levels on distribution feeders and modify the conventional patterns of voltage and current signals. Therefore, what is vital for the functional reliability of synchronous measurements is the implementation of measurement algorithms, which can realize high-accuracy measurements, both in quasi-static and dynamic EPS operating conditions. This article presents the results of software simulations and hardware tests of measurement algorithms that meet the requirements of the IEEE C37.118™-2011 Standard.

Keywords: PMU-based measurements technology, time synchronization, power system operation, reliability, power system adaptive automation

1. Introduction

The availability of high-precision timing sources, such as the Global Positioning System (GPS) and the IEEE 1588 compliant network clock sources [1–3] plus the networking capability [4–5] of protective relaying devices and systems, is fundamentally changing the way that many

current and future protective relaying applications are or will be implemented. Synchrophasor measurements [6–10], i.e., phasor measurements with high-accuracy time stamping, are under consideration for many future protective relaying applications [11–20]. Synchrophasor measurements are also used in many other power system applications such as wide-area monitoring and situational awareness applications. This chapter focuses primarily on their proper physical realization resulting from the standard requirements. Fulfillment of these requirements can lead to the development of the relaying applications that can either be implemented or are considered for future implementations.

The use of high-accuracy measurements and reliable protective algorithms with adequately high-accuracy and prompt decision-making [21–28] should guarantee an effective operation and protection of the electric power systems (EPS) from the consequences of disturbances also in the power system area characterized by changeable operation frequency over a wide range. The adaptation of measurement and protective algorithms in cases under consideration has the frequency nature, i.e., it concentrates on such a change of the parameters of algorithm operation which guarantees the proper estimation of measurement and criterion values by changeable frequency of the input measurement signals: currents and voltages received from the primary circuit [22–23]. The measurement and protective algorithms used at present in the measurement-protection devices tend to be defined for the constant frequency 50/60 Hz of the input signal, and from the point of view of the synchronous measurement standard requirements, they are characterized by too big inaccuracies when the frequency of the input signals varies over a wide range [21–22]. Another problem for the formulation of the measurement algorithms is the determination of the level of the insensitivity of these algorithms to the existence of interfering components in the input signals ([22, 25, 27]). Several interfering components and factors can occur especially in the input measurement signals during the faults within the EPS ([14–15, 22, 25, 27]). This situation is accompanied by high penetration levels of intermittent dispersed generation (DG) [14–15], and it can significantly affect the EPS operation. The existence of thyristor frequency converter is the source of high harmonics, particularly the odd high 5th, 7th, 9th harmonics with the amplitude reaching up to 10% of the amplitude of the basic component [16]. Moreover, as penetration levels increase, concerns regarding dynamic interactions among DG units are becoming more important. Uncontrolled personal electric vehicle (PEV) charging can lead to the overloading of the distribution equipment and violations of low-voltage limits and their courses. Also, the DC component in the input current signals can reach significant values and has a considerable influence on the accuracy of the measuring algorithms [21–22]. In summary the measuring algorithms implemented in the digital measure-protective systems should be characterized by:

- High accuracy of operation over a wide range of frequency change

- Non-sensitivity or low-level sensitivity to the existence of high harmonics in the input measurement signals

- Low inaccuracy in the case of the existence of the DC component of the high level and longtime decay (in current signals)

- Maximum short time of transient states in the measurements or decision-making

2. Basic requirements resulting from the series of the standard C37.118™

The IEEE Std 1344™-1995 was the original synchrophasor standard. It was replaced in 2005 by IEEE Std C37.118-2005 [6]. The newest standard has been split into two standards: IEEE Std 37.118.1-2011 [7], covering measurement provisions, and IEEE Std 37.118.2™-2011 [8], covering data communication. In the IEEE standard from 2011, there is a significant change of the requirements for synchronous measurements and additional clarification for the phasor and synchronized phasor definitions. The concepts of total vector error (TVE) and compliance tests are retained and expanded, tests over temperature variation have been added, and dynamic performance tests have been introduced [7–9]. In addition, limits and characteristics of frequency measurement and rate of change of frequency (ROCOF) measurement have been developed.

Phasor representation of sinusoidal signals is commonly used in the AC power system analysis. The sinusoidal waveform defined in Eq. (7):

$$x(t) = X_m(\omega t + \varphi) \tag{1}$$

is commonly represented as the phasor as shown in Eq. (2) [7]:

$$\underline{X} = X_r + jX_i = \frac{X_m}{\sqrt{2}} e^{j\varphi} = \frac{X_m}{\sqrt{2}} (\cos\varphi + j\sin\varphi) \tag{2}$$

where the magnitude is the root-mean-square (RMS) value, $X_m/\sqrt{2}$, of the waveform and the subscripts r and i signify real and imaginary parts of a complex value in rectangular components. This phasor is defined for the angular frequency ω.

TVE is an expression of the difference between a "perfect" sample of a theoretical synchrophasor [7] and an estimate given by the unit under test at the same instant. The value is normalized and expressed as per unit of the theoretical phasor. TVE is defined in the following Eq. (7):

$$TVE(n) = \sqrt{\frac{\left(\hat{X}_r(n) - X_r(n)\right)^2 + \left(\hat{X}_i(n) - X_i(n)\right)^2}{(X_r(n) + X_i(n))^2}} \tag{3}$$

where $\hat{X}_r$ and $\hat{X}_i$ are the sequences of estimates given by the unit under test and $X_r(n)$ and $X_i(n)$ are the sequences of theoretical values of the input signal at the times (n) assigned by the unit to those values. Synchrophasor measurements shall be evaluated using the TVE criterion of Eq. (3).

A phasor measurement unit (PMU) shall also calculate and be capable of reporting frequency and ROCOF [7]. For this measurement, the following standard definitions are used. If there is given a sinusoidal signal, as in the Eq. (7):

$$x(t) = X_m \cos[\Psi(t)] \tag{4}$$

the frequency is defined as follows:

$$f(t) = \frac{1}{2\pi} \frac{\Psi(t)}{dt} \tag{5}$$

Then, the ROCOF (rate of change of frequency) is defined:

$$\text{ROCOF}(t) = \frac{df(t)}{dt} \tag{6}$$

As mentioned above, the series of the Standard C37.118™ was developed for synchronized phasor measurement systems in power systems. They define a synchronized phasor (synchrophasor), frequency, and rate of change of frequency (ROCOF) measurements. They also describe time tag and synchronization requirements for measurements of all three of these quantities. Next, C37.118™ specifies methods for evaluating these measurements and requirements for compliance with the standard under both static and dynamic conditions. The "old" 2005 version of the standard, commonly followed by equipment manufacturers and system integrators, specifies the performance of phasor measurements only under steady-state conditions. The latest revision of the standard (the 2011 update) extends the synchrophasor definition. It also specifies measurement requirements and test conditions. Steady-state requirements of TVE and ROCOF (resulting from the IEEE C37.118.1–2011 Standard) are included in [7, 9].

The standard C37.118.1–2011 defines the measurement response time and measurement delay time [7]. The measurement response time is the time to transition between two steady-state measurements before and after a step change is applied to the input. The PMU shall support data reporting (by recording of output). This reporting shall be done at submultiples (F_s) of the nominal power-line (system) frequency (**Table 1**) [7].

According to the standard, the support for other reporting rates is optional and includes higher rates like 100/s or 120/s or rates lower than 10/s such as 1/s. The rates lower than 10/s are not subject to dynamic requirements. In this case no filtering is required, and lower-rate data (<10/s) can be provided directly by selecting every nth sample from a higher-rate stream. The reporting rate and performance class are often the largest factors influencing the accuracy of the measurements. These determine the measurement window to be used, filtering, and the length of the interval over which an event will be reported.

To comply with the standard, a PMU shall provide synchrophasor, frequency, and ROCOF measurements that meet the requirements in a given class [7]. These requirements shall be met at all times and under all configurations irrespective of whether the PMU function is a stand-alone physical unit or included as part of a multifunction unit. So, all compliance tests are to be performed with all parameters set to standard reference conditions, except those being varied

System frequency	50 Hz			60 Hz					
Reporting rates (F_s, frames per second)	10	25	50	10	12	15	20	30	60

Table 1. Required PMU reporting rates [7].

as specified for the test. The reference condition specified for each test is the value of the quantity being tested when others are unvarying. Only the parameters specified for each requirement shall be varied as the effects shall be considered independently. Reference conditions for all tests are defined in [7].

3. General characteristics of filtration

The main objective of filtration in the measuring and automation devices within the EPS is to pass signal components lying in a selected frequency band and to suppress signal components of the other frequencies. It is because of the existence of the interfering components in the input signals which can occur especially during faults within the EPS, high penetration levels of intermittent DG, and today's widely used thyristor frequency converters.

Generally, a linear filter can be described by the equation:

$$y(t) = \int_{-\infty}^{\infty} x(t-\tau) \ h(\tau)d\tau \tag{7}$$

where y and x are the output and input signals and h is the response function of the filter.

After the Fourier transform of the Eq. (7) is obtained:

$$Y(j\omega) = X(j\omega) \ H(j\omega) \tag{8}$$

Eqs. (7) and (8), respectively, characterize the filter completely in the time and frequency domain. The function $h(\tau)$ is important for the characteristics of the filter like the function $H(j\omega)$ which represents its frequency spectrum.

In principle, the shorter the interval of the transient state of the filter, the worse the filtration properties. Thus, better filtration properties lead to the extension of time to the stable output response. In practice, it is a trade-off between the short time of the transient state and high quality of filtration, depending on the application requirements. In particular the short transient states of the filtration are required in the power system protection devices. Short stabilization time should be kept in order to take fast and proper decisions during the disturbance, the change of network configuration, the discharge of power, etc. Therefore, it is recommended that filters should be used with fast-decay w-functions or w-functions described in the period T_w and outside this range: taking a value 0. Concluding, filtering of input measurement signals should provide:

- Fast stabilization of output signals after a step change of an input signal (ensuring short time of the measurement)

- Effective elimination or dumping of the interfering (unusable) components

- Possible low computational effort (quasi real-time measurement)

Digital filtration is based on the discrete values of an input signal. Using this technique, a discrete output signal can be obtained and is dependent on the input signal and filter characteristics. The characteristics of the filter can be described using the frequency and time characteristics.

Considering the frequency characteristics of filters, both analog and digital, the following are groups of filters:

- Low-pass filters

- Band-pass filters

- High-pass filters

- Stopband filters

From this group, low-pass and band-pass filters are especially widely used in the power system protection automation.

Analyzing the time characteristics, two groups of digital filters can be distinguished:

- Non-recursive filters of finite impulse response (FIR)

- Recursive filters of infinite impulse response (IIR)

A digital non-recursive filter can be described by Eq. (9):

$$y(n) = \sum_{k=0}^{p-1} a_{(k)} x(n-k) \tag{9}$$

where x and y are the input and output samples, $a_{(k)}$ is the filter coefficients, and p is the number of samples in the window.

Eq. (9) of a non-recursive filter is a discrete convolution of filter coefficients and an input signal, limited to p samples of the input signal.

A digital non-recursive filter can be described by Eq. (10):

$$y(n) = \sum_{k=0}^{p-1} a_{(k)} x(n-k) + \sum_{k=1}^{w} b_{(k)} y(n-k) \tag{10}$$

where $a_{(k)}$ and $b_{(k)}$ are the filter coefficients and w is number of coefficients $b_{(k)}$, $w < (p - 1)$.

Eq. (10) shows that actual response of that filter is not only a function of an input signal and filter coefficients but also a function of w-numbers of the previous values of the output signal. After using the Z-transform, we can obtain:

- For a non-recursive filter:

$$H(z) = \frac{Y(z)}{X(z)} = \sum_{k=0}^{p-1} a_{(k)} z^{-k} \tag{11}$$

- For a recursive filter:

$$H(z) = \frac{Y(z)}{X(z)} = \frac{\sum_{k=0}^{p-1} a_{(k)} z^{-k}}{1 - \sum_{k=1}^{w} b_{(k)} z^{-k}} \tag{12}$$

To obtain the discrete spectra of the filter, the operator z shall be substituted by the equivalent operator $e^{-j\omega\ T_i}$:

- For a non-recursive filter:

$$H^*(j\omega) = \sum_{k=0}^{p-1} a_{(k)} e^{-jk\omega\ T_i} \quad \text{for } \omega < \frac{\pi}{T_i} \tag{13}$$

- For a recursive filter:

$$H(j\omega) = \frac{\sum_{k=0}^{p-1} a_{(k)} e^{-jk\omega\ T_i}}{1 - \sum_{k=1}^{w} b_{(k)} e^{-jk\omega\ T_i}} \quad \text{for } \omega < \frac{\pi}{T_i} \tag{14}$$

where T_i is the sampling period.

Recursive filters are rarely used in power system automation. The cause is a long stabilization time of an output signal after a step change of an input signal and a relatively high sensitivity to the slight changes of values of the coefficients $a_{(k)}$ and $b_{(k)}$.

The possibilities of optimizing non-recursive filters are limited. The optimization due to the required frequency response, the required high dynamics, and the coefficients of the filter and quick transition from band-pass to stopband frequently leads to high-order filters that are difficult to implement in real time. Therefore, optimization of non-recursive filtering should be pursued by selecting the permissible length of the measurement window and possibly a simple form of the coefficients function (coefficients $a_{(k)}$) that define the required spectral characteristics.

4. Experimental setup

In this study, MATLAB with Simulink and Signal Processing Toolbox was used for software simulations. MATLAB is a popular programming language developed by MathWorks [29]. MATLAB can analyze data, develop algorithms, and create models and applications. The Simulink toolbox is a block diagram environment for multidomain simulation and model-based design. It supports simulation, automatic code generation, and continuous test and verification of embedded systems. Simulink provides a graphical editor, customizable block libraries, and solvers for modeling and simulating dynamic systems. It is integrated with MATLAB. It makes it possible to incorporate MATLAB algorithms into models and export

simulation results to MATLAB for further analysis. The Signal Processing Toolbox provides industry-standard algorithms and applications for analog and digital signal processing (DSP). Among other things, it makes it possible to visualize signals in time and frequency domains, compute FFTs for spectral analysis, and design FIR and IIR filters. Algorithms in the toolbox can be used as a basis for developing custom algorithms.

The second stage of this study was performed using microprocessor-based Automatic Relay Test System ARTES 440 II manufactured by KoCoS Company (**Figure 1a**), and a digital fault recorder RZ-40 (**Figure 2**), manufactured by Energotest, with the implemented functionality of a PMU unit (both algorithms and other special functions). The ARTES 440 II [30] is used for carrying out general operating tests and for testing the configured excitation and tripping characteristics of various protection devices, such as distance protection relays, overcurrent
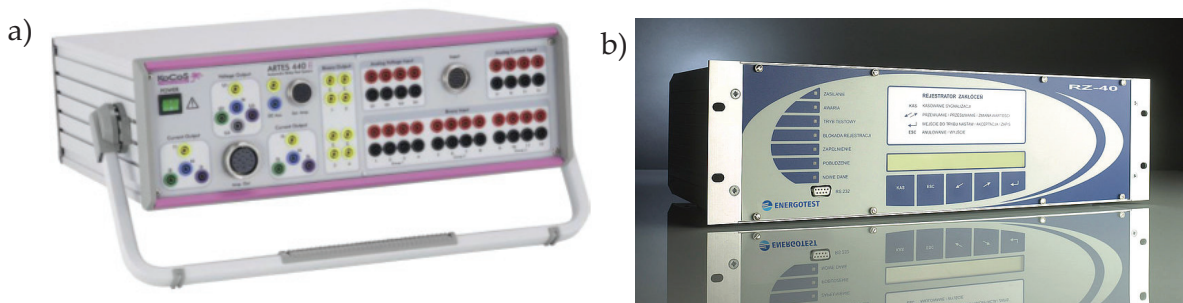

Figure 1. Real photos of (a) ARTES 440 II [30] and (b) RZ-40 fault recorder [31].
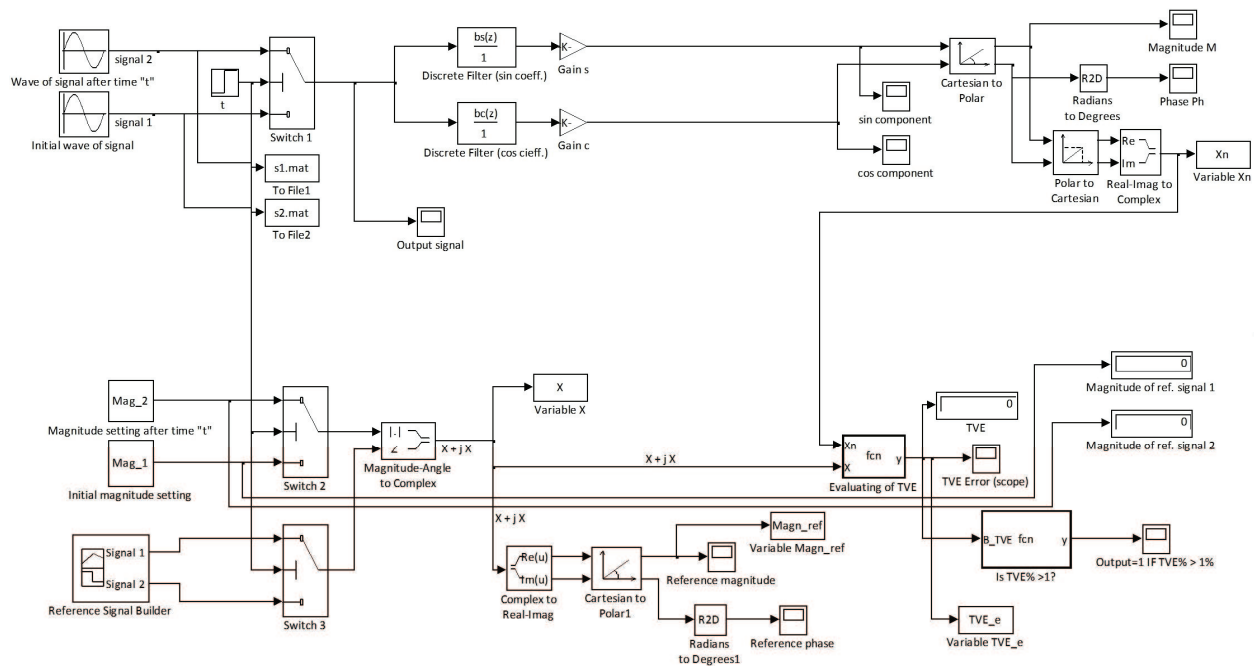

Figure 2. MATLAB/Simulink model used in the software simulations.

relays, and voltage and frequency relays. In addition, the test instrument can also be used as a three-phase function generator which is freely configurable with regard to amplitude, frequency, and phase relation. As mentioned earlier, ARTES 440 II has four voltage and six current amplifiers whose output signals can be set independently from one another as regards amplitude, frequency, and phase angle. The test quantities are calculated from the parameters entered via the software and are supplied to the device under test by means of digital-analog converters and amplifiers. Because the test quantities are generated synthetically, they are unaffected by disturbances in the incoming supply.

The currents generated by the test system are available via the sockets of the current output group. The six current channels are freely configurable as regards phase, amplitude, and frequency. The current amplifiers of the ARTES 440 II provide a maximum test current of 25 A per channel. If higher test currents are required, the amplifier outputs can be operated in parallel. The output values of the current and voltage amplifiers are monitored by the system during tests (internal feedback measurement). If the output values do not agree with the setpoint values, the software issues a warning to this effect. Connections to the device under test are made via safety sockets or a multipole generator output socket. Detailed parameters of the test system are presented in **Table 2**.

Disturbance (fault) recorders have been in use for a number of years and have evolved from analog recording devices to units using digital signal processing and recording techniques. Digital records can be easily collected, transmitted, stored, printed, and analyzed [31]. Also, RZ-40 (**Figure 1b**), a fault recorder selected for this study, typically contains directly measured analog channels, as well as event or binary channels. This allows the recorder to capture the time sequence of analog power system quantities, along with breaker contacts, logic-state changes, event contacts, etc. State-of-the-art recorders typically include calculated analog quantities and logic functions to ensure that pertinent power system information is captured during an event. RZ-40 fault recorder is designed for logging of instantaneous values of voltages and currents as well as binary signals in electric power structures during failures or disturbances. It has many additional functions, e.g., event recorder and electrical value meter. RZ-40 has many functions and wide-open hardware and software structure. Each of the functions can be used independently without lowering parameters of other functions. That is why it was possible to implement additional software and functions of PMUs to fulfill the requirements of the IEEE the C37.118™ series of the Standard.

| General	Frequency range	DC to 3 kHz	Phase angle	0 to 360°
	Transient signals	**DC to 4 kHz**	**Phase resolution**	**0.001°**
	Frequency resolution	**0.001 Hz**	**Phase accuracy**	**Error < ±0.1°**[1]
	Frequency accuracy	**Error < ±0.01%**		
Voltage amplifiers	Resolution THD	13 mV < 0.05%[1]	Accuracy	Error < ±0.05%[1]
Current amplifiers	Resolution THD	1 mA < 0.05%[1]	Accuracy	Error < ±0.05%[1]

[1]For the frequency range of 10 to 200 Hz.

Table 2. Detailed accuracy and resolution parameters of the analog outputs of ARTES II [30].

The other benefit of using this digital fault recorder to realize the functions of PMUs is the fact that many of them are already working (especially in the Polish Power Grid infrastructure). Thus, the implementation of synchronous measurements using these devices will have low hardware costs of the initial wide-area measurements infrastructure. The only thing which needs to be done is to update the software of the functioning devices to the newest one which has the optimized and modified algorithms realizing the PMU functionality. Additionally, existing and future infrastructure facilitates making long-term pilot programs. These programs can lead to the development of new and long-awaited functions to ensure high-power grid availability, stability, and reliability, especially in the power system automation scope. There-fore, the main objective of this study is to initially check the PMU properties of this device according to the IEEE the C37.118[TM] series of the Standard.

4.1. Software simulations in MATLAB

The first stage of the study was to work out a model in MATLAB/Simulink environment (**Figure 3**). This model was used to simulate various tests according to the requirements of C37.118[TM] series of the Standard, especially C37.118.1–2011 [7–9]. It has been used exclusively for research and teaching purposes to demonstrate the properties of orthogonal filters.

On the basis of several other considerations and analyses, e.g., [21–22], full-cycle filters with sine and cosine widows were implemented. Because of the necessity to evaluate TVE (Eq. (3)), there is a reference signal builder in the simulator. The magnitude, phase, and frequency of input signals are freely configurable. The step output "t" is used to switch from signal 1 to signal 2 after a configured time t. Signals 1 and 2 are taken out to Files 1 and 2, a full signal sequence is visible on the scope "Output signal." A generated signal sequence is delivered to the full-cycle filters block with sine and cosine windows. The required coefficients are loaded from MATLAB workspace according to the frequency of the time window. Then, the orthogo-nal components are used to compute magnitude (M) and phase (Ph). Calculated values of the magnitude and phase (in complex variable X_n) are delivered to the function block "evaluating of TVE." The slope of TVE can be viewed on the scope and is exported to variable TVE_e. Additionally, the B_TVE function block is used for evaluation purposes if TVE is below its reference value of 1%. The model presented in **Figure 2** does not have the ROCOF
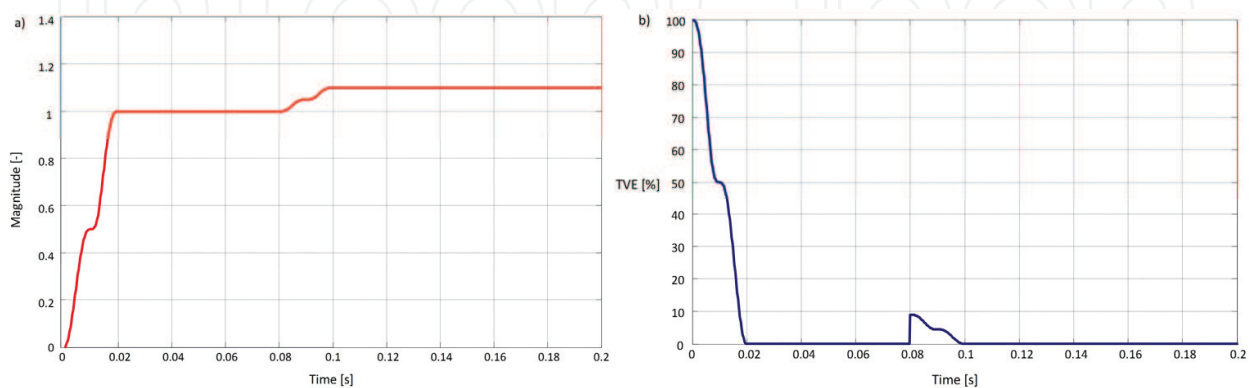

Figure 3. Magnitude and TVE course after a step change of the magnitude in t = 80 ms (a) magnitude course and (b) TVE course.

measurement module. Although the implementation of ROCOF measurements poses no problems (and indeed this was done), the main tests in the dynamic conditions were carried out on a real hardware device, and only a simplified model is presented in **Figure 2**.

Several testing conditions have been simulated using the developed model. Sample results of these tests are presented in **Figures 3** to **6**. All simulations were realized for the sampling frequency f_s = 4 kHz. **Figure 3** presents magnitude and the evaluated TVE course after a step change of input signal magnitude of +10% (in relative values), for the nominal frequency of input signal (f_1 = 50 Hz) and the window frequency of filter (f_w) equal to the nominal frequency. This step change was performed in 80 ms from the beginning of simulation.

Figure 4 shows the courses of TVE for the same f_1 and f_w parameters as before: there is no change of the magnitude, but there is a step change of phase of $\pi/6$ (**Figure 4a**) and $5\pi/6$ (**Figure 4b**) radians. Next, again f_i and f_w are equal to 50 Hz: there is no change of the magnitude and phase, but there is a step change of frequency of -0.5 Hz (**Figure 4c**) and -1 Hz (**Figure 4d**). Finally, **Figure 5** shows the situation, when the frequency of the filter window (f_w = 48.78 H) is almost fully correlated with the frequency of the input signal ($f_1 = f_w$ = 48.78 Hz (**Figure 5a**)) and closely correlated (f_1 = 48.5 Hz, f_w = 48.78 (**Figure 5b**)). Of course for the last test, the coefficients of the filter are different from the first three tests and evaluated and loaded from the MATLAB workspace. In the example, for the selected frequency f_w = 48.78 Hz, there are 82 samples in the filter window, and the filter window is almost
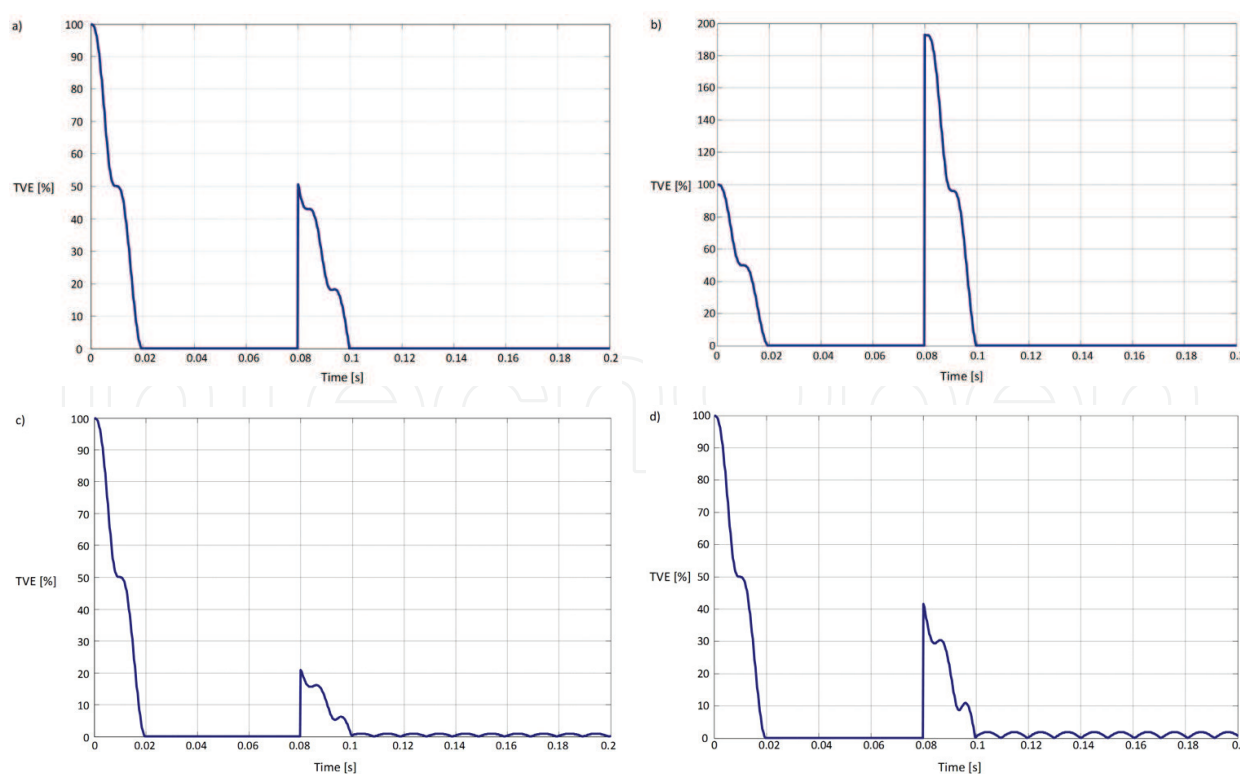
Figure 4. TVE courses after a step change in t = 80 ms of the input signal: (a) phase of $\pi/6$ radians, (b) phase of $5\pi/6$ radians, (c) frequency of 0.5 Hz, and (d) frequency of 1 Hz.
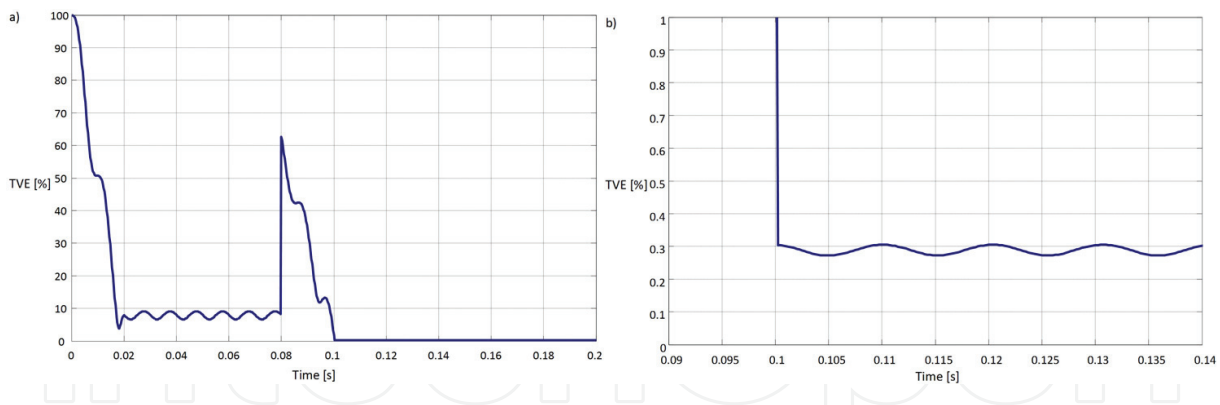
Figure 5. TVE courses for filter window frequency f_w = 48.78 Hz and the input signal of frequency: (a) f_1 = 48.78 and (b) f_1 = 48.5 (zoomed).

fully matched to the frequency of the input signal also equal to 48.78 Hz. The number of samples is a natural number.

Therefore, taking the sampling frequency of 4 kHz, the other two nearest frequencies of the fundamental component of an input signal, for which the window filter can be almost fully correlated with the input signal, are 49.28 (81 samples in the filter window) and 48.19 (83 samples in the filter window). It should be emphasized that this phenomenon is dependent on the sampling frequency. When the sampling frequency is 2 kHz, there are 40 samples in the window (for the frequency of the fundamental component equal to 50 Hz). The nearest two natural numbers of samples are 39 and 41. Evaluating 2000/39 gives the frequency of the window equal to 51.28 Hz and 2000/41 gives f_w = 48.78 Hz. Comparing these frequencies with the ones for f_s = 4 kHz (relatively 50.63 Hz and 49.28 Hz), it can be noticed that lowering the sampling frequency leads to wider frequency ranges in which the algorithm works with the nonmatched frequencies of windows and generates inaccuracies exceeding the limits defined by the standard. On the other hand, raising the sampling frequency leads to the increase in the computational effort and time.

Analyzing software simulations, it can be seen that for the assumed sampling frequency, TVE exceeds the limit of 1% for the frequencies differing from the nominal more than about 0.5 Hz. Therefore, the adaptive technique using switching between filter windows frequencies can be considered to comply with the standard limitations as well as with other solutions described in [21–22].

4.2. Testing and validation of the RZ-40 device by ARTES II

Figures 6–8 show sample hardware tests carried out with the ARTES II and RZ-40 devices. These tests were realized for various conditions and cases described in the IEEE C37.118.1–2011 Standard.

Each of the tests is realized in 1 second. In the half of this period (500 ms from the beginning of test), there is a step change of the given quantity. **Figure 6** shows the courses of the magnitude
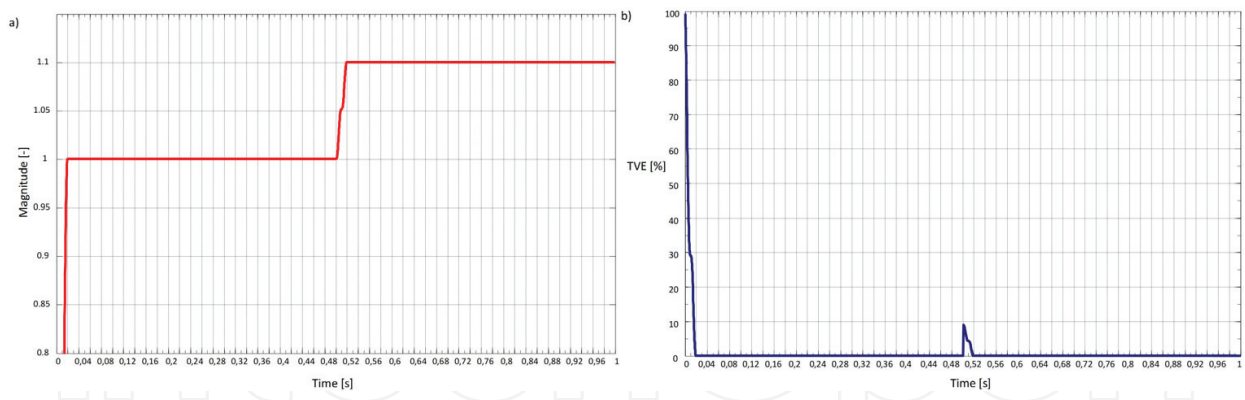
Figure 6. Magnitude and TVE course after a step change of the magnitude in t = 500 ms: (a) magnitude recorded in RZ-40 device and (b) TVE course (evaluated).
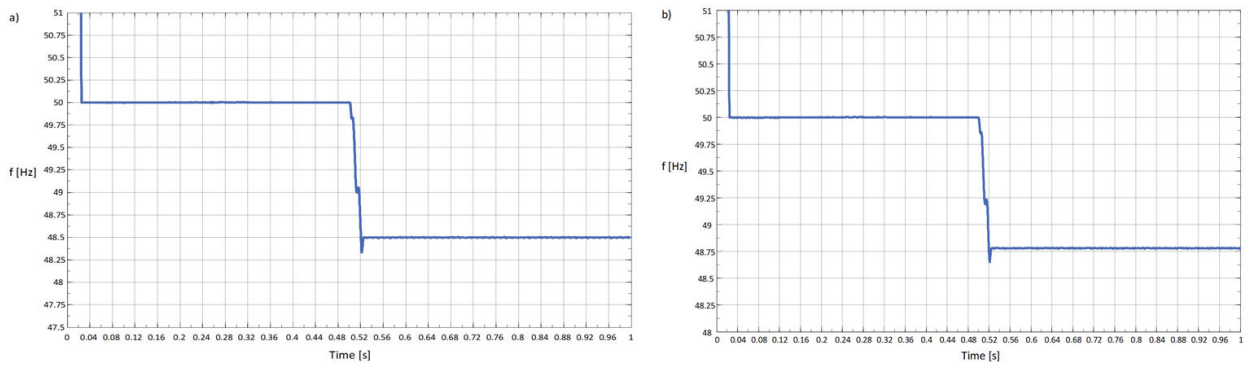
Figure 7. Frequency courses evaluated in RZ-40 device after a step change of the input signal frequency in t = 500 ms: (a) f_1 = 45.5 Hz and (b) f_1 = 45.78 Hz.
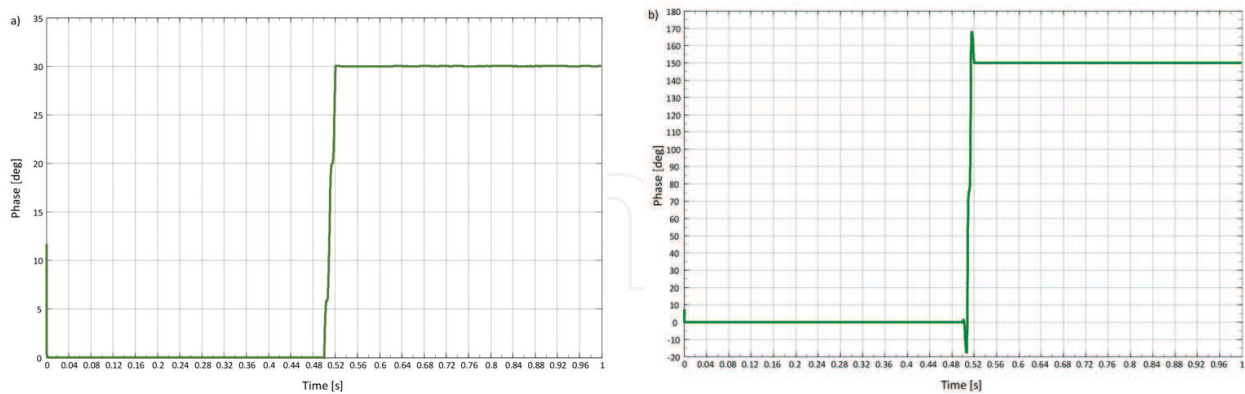
Figure 8. Phase courses recorded in RZ-40 device after a step change of the input signal phase in t = 500 ms: (a) from 0 to 30° and (b) from 0 to 150°.

(**Figure 6a**) and TVE (**Figure 6b**) during the step change of that first on the level + 10% (relative values). The first course is recorded using the disturbance recorder ability implemented in the ET Manager software supplied by the manufacturer. The TVE is evaluated using the recorded

values. **Figure 7** presents the evaluated frequency for 48.5 Hz (**Figure 7a**) and 48.78 (**Figure 7**b). Lastly, **Figure 8** shows the phase courses for the step change of phase from 0 to 30° (**Figure 8a**) and from 0 to 150° (**Figure 8b**).

As it can be observed, there are full-cycle window filters implemented in the RZ-40 devices. It can be concluded from the time period between the occurrence of a step change (0.50 s) and the moment of the stable response to this step (0.52 s). Any fluctuations in the initial period of tests should not be considered as they are the results of transient states of starting simulations (MATLAB/Simulink) or transients after injecting voltages on the RZ-40 inputs when the previous input magnitude was 0.

As mentioned previously, the RZ-40 has been tested in accordance with the C37.118.2011™ Standard and the "2014" amendment. In particular, the implemented measurement algorithms focused on providing high accuracy and stability of frequency determination across a wide range of frequency changes in measurement signals. **Tables 3** and **4** show the results of frequency estimation for a monoharmonic signal with set fundamental frequencies (45 to 55 Hz in 1 Hz steps) for successive 50 samples. Similar measurements were made for further 100 and 200 samples. The results of the measurements are shown in **Figures 9** and **10**. Based on the obtained results, it can be stated that the algorithm is characterized by high-frequency estimation accuracy (average error of measurement below 2 mHz) and high stability (maximal standard deviation at 1 mHz for the extreme frequency of the tested range). The dynamic tests

	45 Hz	46 Hz	47 Hz	48 Hz	49 Hz	50 Hz
Frequency (mean) [Hz]	44,998,237	45,998,779	46,999,410	47,998,901	48,999,969	49,999,111
Standard deviation [mHz]	0,894	<0,001	0,840	<0,001	<0,001	0,415
Mean freq. Error [mHz]	−1763	−1221	−0,590	−1099	−0,031	−0,889
Average percentage error [−]	−0,004	−0,003	−0,001	−0,002	<0,001	−0,002

Table 3. Results of frequency estimation in the RZ-40 for the 50 successive samples (1).

	51 Hz	52 Hz	53 Hz	54 Hz	55 Hz
Frequency (mean) [Hz]	50,998,157	51,999,145	52,998,279	53,999,208	54,998,621
Standard deviation [mHz]	0,395	0,000	0,395	0,344	0,720
Mean error [mHz]	−1843	−0,855	−1721	−0,792	−1379
Average percentage error[−]	−0,004	−0,002	−0,003	−0,001	−0,003

Table 4. Results of frequency estimation in the RZ-40 for the 50 successive samples (2).

performed indicated excellent properties of the algorithm for potential applications in the power system. The results obtained have also been confirmed by independent tests carried out at the Fraunhofer Institute in Magdeburg using a reference device[1].

Synchrophasor measurements should be synchronized with the UTC time with the accuracy sufficient to meet the accuracy requirements of the C37.118 Standard [3]. Time-stamp error should be of just a few (single) μs. In order to fulfill this requirement, the accuracy of the time source should be about ten times higher than the level of the expected time error. To synchronize the RZ-40 unit, the GPS receiver EM-406A and then EM-506 was taken as the source of the time signal. The EM-406A is a 20-channel GPS receiver, and the EM-506 one is a 48-channel receiver. High accuracy of measurements and high precision of time stamps make it possible to develop many new or improved applications. One of them is the SmartLoad system [13, 31].
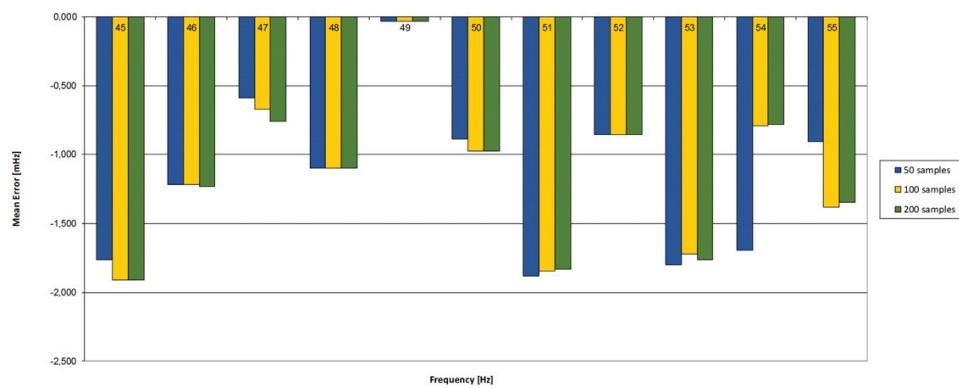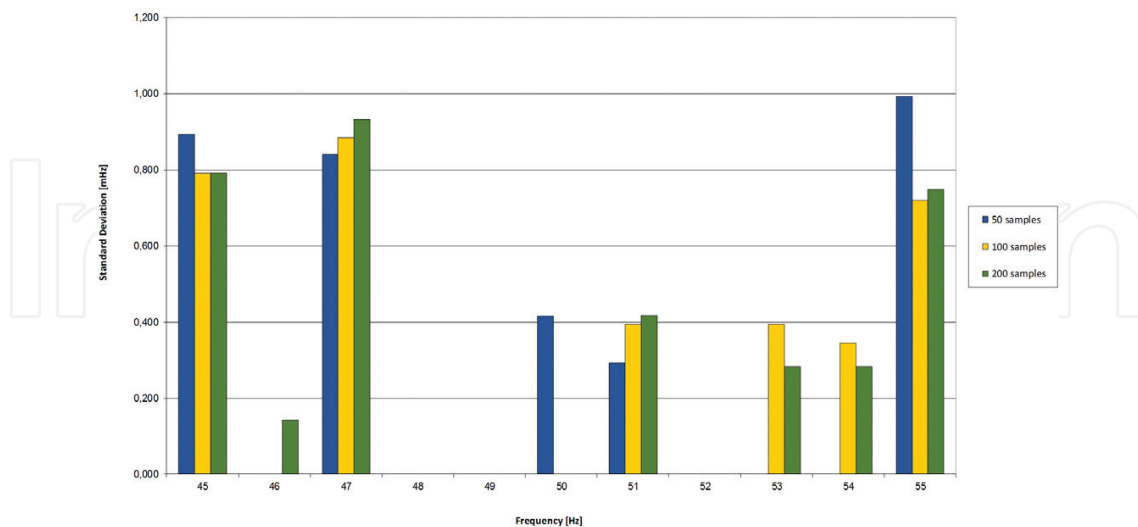

Figure 9. Mean error of frequency estimation.

Figure 10. Standard deviation of frequency estimation.

---

[1]Tests commissioned by Energotest Sp. z o.o.

This system is an advanced system designed to make a quasi real-time balance of power and adaptive load-off in the case of a possible active power deficit in the supervised area of a power network. This system has already been implemented. Some new implementations are under development and will be the subject of subsequent publications. It seems that they can significantly improve the reliability of the power system's operation with the benefits of a well-implemented PMU-based measurements technology.

5. Discussion and conclusions

The IEEE C37.118.1.2011 Standard defines a phasor measurement unit (PMU), which can be a stand-alone physical unit or a functional module within another physical unit. The Standard does not specify any hardware, software, or a method for computing phasors, frequency, or ROCOF. In all likelihood the best solution, especially in the initial period of implementation, is to incorporate the PMU functionality into the existing hardware devices commonly used in the power grid. This minimizes costs and facilitates realizing potential pilot programs. The pilot programs seem to be the essential part of the PMU and synchronous measurement studies. Considering the RZ-40 unit is by no means accidental. This unit has a modular and scalar hardware architecture. It is very easy to change the input analog cards, DSP module, and communication module or to update the firmware of the unit including the measurement algorithms and other functionalities [28]. Last but not least, it is also a very popular unit in the Polish Power Grid.

Analyzing the requirements for the synchronous measurements resulting from the C37.118™ series of the Standard, significant changes can be noticed between the 2005 and 2011 versions. The requirements in the version of the Standard dated 2005 were defined only for static conditions and were very imprecise. This leads to their free interpretation by manufactures because several of them were not directly defined or defined on the levels which give many different solutions allowing compliance with the Standard. Although many algorithms which are used may comply with the 2005 Standard, they may have different properties in the dynamic stages, especially during the fast transient states. That is why the Standard from 2011 emerges. It is much more precise, and it defines the requirements both in the static and dynamic conditions. It also defines many important time limits for the measurement algorithms realizing synchronous measurements. It was concluded that the compliance problems with the Standard in the case of wide-area measurements are dependent on their target applications. It was almost impossible to build the wide-area protection systems based on the Standard of 2005. As a matter of fact, it defined some practical requirements in steady conditions, but it is the requirements in dynamic states that are most vital for the protections. In addition these "dynamic" requirements should be comparable in different devices realizing PMU functions. All this makes synchronous measurements very hard to realize, mainly as regards factors related to the PMU-expected higher functionalities. Simulations realized in this study indicate the possibility of developing fast and reliable adaptive measurement algorithms to comply with the C37.118.1–2011 requirements. Several tests confirm that for the RZ-40 device. Detailed analyses of the 2011 Standard point that some of the requirements are very hard or even impossible to meet. Some of the difficulties in meeting the requirements probably

result from simple typo-errors they contain. Other requirements are feasible but hard to implement. They cause computational problems resulting from increasing the response time and error on the output. This seems to be confirmed by Amendment 1 to the Standard released at the end of March 2014 [9] entitled "Modification of Selected Performance Requirements," in which many of the required parameters, mainly applying to the dynamic requirements, are revised. It should be emphasized that most of these parameters were met by the RZ-40 during the tests discussed in this study for limits defined in 2011. Summing up, on the basis of the tests defined in the Standard and conducted in this study, it is possible to meet the Standard requirements by the devices like RZ-40. It should be observed that these are "synthetic tests" and probably many other devices can comply with the Standard. On the other hand, most of these "others" were only tested and confirmed by the manufacturers to comply with the standard of 2005. Therefore, long-term pilot tests are essential to compare the properties of different devices with the PMU functionality. These tests should be conducted using different PMU devices working in the same locations of the power grid. The initial forecasting time of such tests is from about 6 months to a year. Further research is needed to analyze the results. Some of the most noticeable changes to the power distribution landscape are being driven by the proliferation of intermittent DG, PEVs, microgrids, and power electronic components. The application of PMUs in distribution systems is still under-explored or is at the implementation stage. This is mostly due to the recognized technical problems (explained and revised in this study) and economic factors. However, since the drivers of change and needs for implementation are rapidly increasing, there is a growing interest in applying PMUs in the EPS, which will consequently engender a new body of research.

Acknowledgements

Author details

Michał Szewczyk

Address all correspondence to: michal.szewczyk@polsl.pl

Silesian University of Technology, Gliwice, Poland

References

[1] IEEE Std 1588™-2008. IEEE Standard for a Precision Clock Synchronization Protocol for Networked Measurement and Control Systems

[2]   PC37.238. IEEE Draft Standard Profile for Use of IEEE 1588 Precision Time Protocol in Power System Applications

[3]   Szewczyk M. Time synchronization for synchronous measurements in electric power systems with reference to the IEEE C37.118TM standard - selected tests and recommendations. Przegląd Elektrotechniczny. 2015;**4**:144-148. DOI: 10.15199/48.2015.04.32

[4]   Szewczyk M. Selected analyses of teletransmission and teleinformatic structures in electrical power. Przegląd Elektrotechniczny. 2014;**3**:1-5. DOI: 10.12915/pe.2014.03.1

[5]   Szewczyk M. Analysis of the requirements of reliability and quality for systems and data transmission equipment in modern power systems. Przegląd Elektrotechniczny. 2014;**3**:84-89. DOI: 10.12915/pe.2014.03.1

[6]   C37.118 rev. IEEE Standard for Synchrophasor Measurements for Power Systems. 2005

[7]   C37.118.1 rev. IEEE Standard for Synchrophasor Measurements for Power Systems. 2011

[8]   C37.118.2 rev. IEEE Standard for Synchrophasor Measurements for Power Systems. 2011

[9]   IEEE Standard for Synchrophasor Measurements for Power Systems, Amendment 1. Modification of Selected Performance Requirements. 27 March, 2014

[10] Szewczyk M. Standard requirements for systems realizing synchronous measurements in the power system infrastructure. Przegląd Elektrotechniczny. 2014;**3**:80-83. DOI: 10.12915/pe.2014.03.16

[11] Wache M, Murray DC. Application of Synchrophasor measurements for distribution networks. IEEE Power and Energy Society General Meeting. Jul. 2011:1972-1975

[12] Sanchez-Ayala G, Aguerc JR, Elizondo D, Lelic M. Current trends on applications of PMUs in distribution systems, innovative smart grid technologies (ISGT). 2013. IEEE. Feb. 2013;**24-27**:1-6

[13] Szewczyk M. Conditions for the improvement and proper functioning of power system automation equipment in the present and the expected future structure of the electric power sector. Przegląd Elektrotechniczny. 2015;**5**:179-186. DOI: 10.15199/48.2015.05.40

[14] Halinka A, Szewczyk M. Distance protections in the power system lines with connected Wind Farms. Gesche Krause, editor. From Turbine to Wind Farms - Technical Requirements and Spin-Off Products. InTech; April 2011:135-160. DOI: 10.5772/15955

[15] Halinka A, Rzepka P, Szablicki M, et al. Impact of proper functioning of power system automation for the safety of power system in the consideration of the new technical and economical solutions in polish power grid. Przegląd Elektrotechniczny. 2011;**2**:140-143

[16] Borghetti A, Nucci CA, Paolone M, Ciappi G, Solari A. Synchronized phasors monitoring during the islanding maneuver of an active distribution network. IEEE Transactions on Smart Grid. March 2011;**2**(1). Article number 5680630:70-79

[17] Meng W, Wang X, Wang Z, Kamwa I. Impact of causality on performance of Phasor measurement unit algorithms. IEEE Transactions on Power Systems. 2017:1-11. DOI: 10.1109/TPWRS.2017.2734662

[18] Roscoe AJ, Burt GM, McDonald JR. Frequency and fundamental signal measurement algorithms for distributed control and protection applications. IET Generation, Transmission and Distribution. 2009;**3**(5):485-495

[19] Kundu P, Pradhan AK. Wide area measurement based protection support during power swing. International Journal of Electrical Power & Energy Systems. December 2014;**63**:546-554. DOI: 10.1016/j.ijepes.2014.06.009

[20] Shima KS, Kimb ST, Leec JH, et al. Detection of low-frequency oscillation using synchrophasor in wide-area rolling blackouts. International Journal of Electrical Power & Energy Systems. December 2014;**63**:1015-1022. DOI: 10.1016/j.ijepes.2014.06.069

[21] Rebizant W, Szafran J, Wiszniewski A. Digital Signal Processing in Power System Protection and Control. Springer-Verlag London; 2013. DOI: 10.1007/978-0-85729-802-7

[22] Halinka A., Sowa P, Szewczyk M. Measurement algorithms of selected electric parameters in wide range of frequency change. Proc. of SIP2001. Honolulu. USA: 155–159

[23] Kamwa I, Samantaray SR, Joos SR. Wide frequency range adaptive phasor and frequency PMU algorithms. IEEE Transactions on Smart Grid. March 2014;**5**(2). Article number 6575186:569-579

[24] Chakir M, Kamwa I, Le H. Extended C37.118.1 PMU algorithms for joint tracking of fundamental and harmonic phasors in stressed power systems and microgrids. IEEE Transactions on Power Delivery. June 2014;**29**(3). Article number 6810880:1465-1480

[25] Phadke AG, Kasztenny B. Synchronized phasor and frequency measurement under transient conditions. IEEE Transactions on Power Delivery. 2009;**24**(1):89-95

[26] Roscoe AJ, Burt GM, Rietveld G. Improving frequency and ROCOF accuracy during faults, for P class Phasor measurement units. 2013 IEEE International Workshop on Applied Measurements for Power Systems, AMPS 2013 – Proceedings 2013. Article number 6656233. 97–102

[27] Premerlani W, Kasztenny B, Adamiak M. Development and implementation of a synchrophasor estimator capable of measurements under dynamic conditions. IEEE Transactions on Power Delivery. January 2008;**23**(1):109-123

[28] A Study of the Measurement-Path Accuracy of Digital Protection Devices in a Wide Range of the Frequency Change. Unpublished report of the research project sponsored by the Polish National Research Committee. Research manager of the project: Michał Szewczyk

[29] www.mathworks.com

[30] www.kocos.de

[31] www.energotest.com.pl